Monitoring Accropodes Breakwaters using RGB-D Cameras

Monitoring Accropodes Breakwaters using RGB-D Cameras

D. Moltisanti[1], G. M. Farinella[1], R. E. Musumeci[2], E. Foti[2] and S. Battiato[1]
[1]*Image Processing Laboratory, University of Catania, Viale Andrea Doria 6, Catania, Italy*
[2]*Department of Civil Engineering and Architecture, University of Catania, Viale Andrea Doria 6, Catania, Italy*

Keywords: 3D Breakwaters Monitoring, RGB-D Cameras, Iterative Closest Point, Point Cloud Alignment.

Abstract: Breakwaters are marine structures useful for the safe harbouring of ships and the protection of harbours from sedimentation and coasts from erosion. Breakwater monitoring is then a critical part of coastal engineering research, since it is crucial to know the state of a breakwater at any time in order to evaluate its health in terms of stability and plan restoration works. In this paper we present a novel breakwaters monitoring approach based on the analysis of 3D point clouds acquired with RGB-D cameras. The proposed method is able to estimate roto-translation movements of the Accropodes, building the armour layer of a breakwater, both under and above still water level, without any need of human interaction. We tested the proposed monitoring method with several laboratory experiments. The experiments consisted of the hitting of a scale model barrier by waves in a laboratory tank, aiming to asses the robustness of a particular configuration of the breakwater (that is, the arrangement of the Accropodes building the structure). During tests, several 3D depth maps of the barrier have been taken with a RGB-D camera. These point clouds, hence, have been processed to compute roto-translation movement, in order to monitor breakwater conditions and estimate its damage over time.

1 INTRODUCTION

RGB-D cameras are nowadays used in a lot of applications which spread over many purposes. In this paper we use such cameras in a hydraulic engineering context with the goal of monitoring the status of a Accropode breakwater attacked by waves. During an experiment a scale model barrier is hit by waves in a laboratory tank, aiming to asses the robustness of a particular configuration of the breakwater. Several 3D models of the barrier are acquired throughout the test with a RGB-D camera, in order to monitor the conditions of the breakwater and estimate its damage over time through Computer Vision algorithms.

To compute the shifts of the Accropodes occurred during an experiment, we use as reference a 3D model of the barrier taken at the beginning of the experiment. From this 3D model we extract a set of control points used to estimate roto-translational movements in local regions of the barrier. Every control point defines a portion of the breakwater and Accropodes shifts are computed by performing radius searches on the spherical neighbourhoods of such points.

The rest of the paper is organized as following. In Section 2 the motivations of this work are given. Section 3 provides an overview of the setup in which tests have taken place, also describing the involved experimental scenario. In Section 4 we analyse the proposed approach, whereas Section 5 discusses the experimental results. Finally, Section 6 provides conclusions and hints for future works.

2 MOTIVATIONS OF THE WORK

Rubble mound breakwaters play an important role in the protection of ports or beaches from wave attacks. Indeed, by inducing wave breaking on the structure, they allow to dissipate a great portion of the incident wave energy, generating several beneficial effects, such as the control of wave height within harbour basin, reduction of the impacts of storms along the coasts, minimisation of coastal erosion, etc.

The armour layer of the rubble mound breakwater, i.e. the external layer of large blocks facing offshore, is the most important part of the structure. Depending on the structure function, wave conditions, material availability and breakwater shape, the armour layer may be built by using natural stony blocks or artificial concrete blocks. Amongst the artificial blocks, one of the most used is the Accropode (Kobayashi and Kaihatsu, 1984), which has been proposed by Sogreah

Moltisanti D., Farinella G., Musumeci R., Foti E. and Battiato S..
Monitoring Accropodes Breakwaters using RGB-D Cameras.
DOI: 10.5220/0005297000760083
In *Proceedings of the 10th International Conference on Computer Vision Theory and Applications* (VISAPP-2015), pages 76-83
ISBN: 978-989-758-089-5

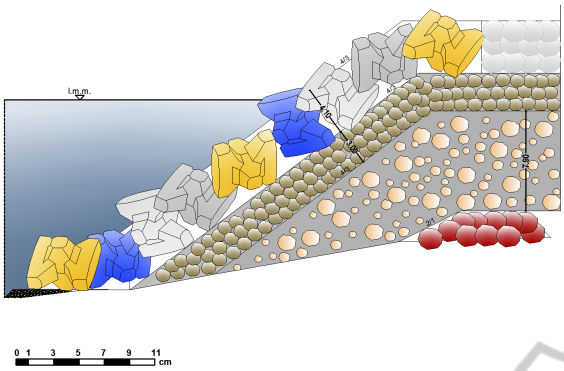

Figure 1: Schematic section of one configuration of the 2D breakwater model, where the armour layer is made up by Accropode blocks.

in 1981. Such kind of blocks is often used to build coastal structures, thanks to the interlocking properties which guarantees an high stability, when both a large mass of the block and a steep slope of the structure are required (Van der Meer, 1987; Kobayashi and Kaihatsu, 1984).

The action of the waves during storms may damage the armour layer of rubble mound breakwaters and this can importantly compromise the overall stability of the structure. Due to the complexity of the problem, neither analytical nor numerical predictions are able to provide damage estimates, and coastal engineers rely on the results of laboratory experiments carried out on properly scaled physical models to assess the level of damages under known wave conditions.

Traditionally, at field site, breakwaters are visually inspected using limited, qualitative and subjective methods, like underwater video monitoring effectuated by professional scuba divers, which entails both cost and security issues. Also, traditional underwater monitoring systems require expensive devices, like acoustic beams emitters or laser scanner (Auld, 2010; Caimi and Kocak, 1997). An interest in reducing such costs is growing up over time: relatively low cost devices like RGB-D cameras, for instance, have more and more resolution, whilst the related supporting Computer Vision algorithms are increasingly precise. Additionally, RGB-D cameras can see both under and above the water, combining so in only one device the capability to observe the whole structure. The development of new Coastal Engineering systems based on low cost solutions with a high accuracy level is then a new challenge for Computer Vision. The proposed breakwater monitoring method is particularly focused on this context, since it requires affordable devices (indeed, we used a Microsoft Kinect).

Using an automated methodology allows also to investigate a bigger amount of data, that is more experimental results to be analysed. Our method requires only a minimal user interaction via a friendly graphic interface for the alignment phase of the point clouds. Furthermore, this is a stage which has to be done only after the experiment: the only operation which engineers must care about is the proper location of the RGB-D camera for the acquisition of the 3D models from an appropriate point of view.

3 EXPERIMENTS SETUP

The experimental campaign has been carried out at the Hydraulic Laboratory of the University of Catania within an experimental wave tank, which is equipped with an electronically controlled flap-type wavemaker, able to produce both regular and irregular water waves. The wave tank is 18m long, 3.6m wide and 1.0m high. In order to test the proposed approach, the stability of a rubble mound breakwater with the armour layer made up by artificial Accropode blocks has been investigated. Such a structure is inspired by a real structure to be built in the Eolian Islands to protect an existing marina, by using a scale 1:80 between the model and the prototype. In particular, during the present experiments only a section 1m wide of the tank has been used, in order to better control both the construction and the stability of the two-dimensional structure. Figure 1 shows a section of the model of the breakwater, where it can be noticed the armour layer made up by Accropodes, while the underlying layers, starting from the filter and going down to the core of the structure, are made up by natural stones. The Accropode blocks were built on purpose by using a mixture of a resin, basaltic sand and iron powder in order to obtain the desired density. The side of the Accropode was 4.64 centimetres. It should be noted that Accropodes are painted. This has been done in order to reduce scale effects related to the different roughness we have at prototype scale and at model scale. The different colours used helped also to identify the movement of each single Accropode.

The RGB-D camera is positioned on a specific stand supported by a scaffolding in front of the structure at a distance of approximately 1.2m from the toe of the structure, in order to be able to recover the entire structure, both above and below water level.

Several irregular wave conditions, corresponding to different stages of the design storm, have been run in order to test the stability of the armour layer. After each wave conditions, a depth map of the armour layer was obtained by stopping the wavemaker, but

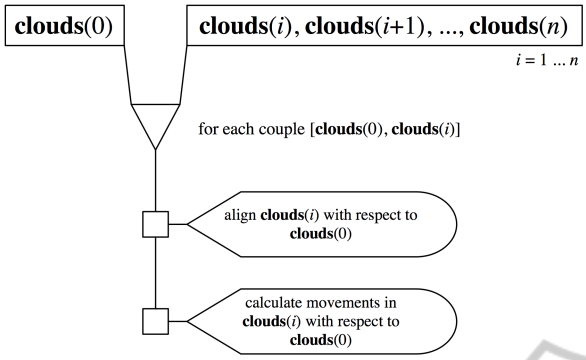

Figure 2: Workflow of the proposed approach.

without empting the wavetank. Indeed the emptying and filling of wavetanks, which is often performed in hydraulic laboratories to obtain clear pictures, is a time-consuming task which in some cases may even perturb the stability of the structure itself.

4 PROPOSED APPROACH

Before starting to expose the proposed approach, we first define a simple notation to refer to the 3D models of a test sequence. We call "clouds" the ordered list of meshes that have been reconstructed during an experiment: at position *i* of the clouds list is stored the *i*-th 3D model captured at time *i*. A special cloud is the one stored at position 0: this is the mesh of the barrier at the initial condition, that is before the experiment started. We use the cloud at time 0 as reference mesh to evaluate movements in every subsequent cloud at time *i*-th.

The pipeline of our method is reported in Figure 2. Since the barrier is hit by waves throughout the experiment, the Accropodes are subject to roto-translation movements over time: to evaluate these shifts we compare every cloud *i*-th with the reference clouds(0). The first step we run is the alignment of the cloud *i*-th with respect to the reference cloud, as discussed below. Thereafter, we evaluate Accropodes movements by calculating local differences between the point clouds, as explained in Subsection 4.2.

4.1 Point Clouds Alignment

Although the Kinect employed in the proposed system has been fastened to a rigid bar, it may happen that two 3D models belonging to the same testing sequence are not aligned, that is the models don't overlap exactly one with the other. This can occur due to slight vibrations transmitted to the Kinect by the waves during the experiment, causing thus little shifts of the camera.

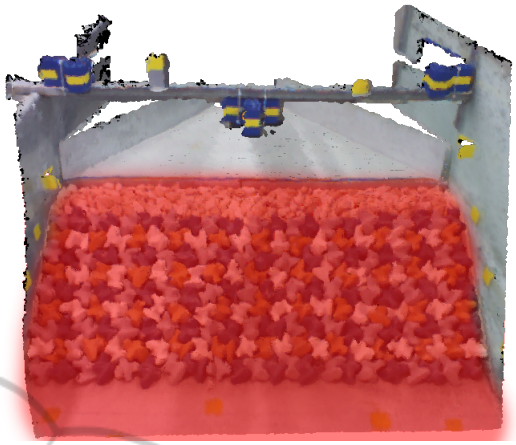

Figure 3: Region of a cloud where movements can take place (marked in red).

We align every clouds(*i*) of the test sequence with respect to the reference clouds(0). We use the Iterative Closest Point algorithm (Chen and Medioni, 1992) to align the clouds by considering specific sub-clouds selected by the user on the reference mesh. A sub-cloud is a mesh composed of sub-sets of points of the source cloud; in particular, we are interested in picking those parts of the clouds where no movements can occur (for instance, the bar upon the barrier, or the wall limiting the Accropodes). We call this sub-cloud "icp-cloud": icp-cloud(0) refers then to the sub-cloud of the reference clouds(0), while icp-cloud(*i*) refers to the *i*-th cloud of the sequence.

Given that ICP operates by finding matches between points and minimising their distance, a region where some movements take place would lead to a failure of the alignment algorithm. In Figure 3 we can see an example of such region, marked in red. In this part of the cloud are located the Accropodes, which move both slightly and considerably, according to the intensity of the flooding waves. You might notice that the steel rod at the bottom of the barrier is marked too; this is because it could happen that some Accropodes fall down and get to the bottom due to a barrier break. In these cases, if we were considering those part for the alignment, we would cause the failure of the ICP procedure as the matching between the reference mesh and the cloud to be aligned would fail.

In Figure 4 we can observe the building phase of the icp-cloud. The software asks the user to pick some spheres from the reference clouds(0): the points lying inside the red spheres are extracted from the source cloud and put in the icp-cloud. We build the sub-cloud asking the user only once per test sequence. Specifically, we build the icp-cloud on the reference

clouds(0): then, for every clouds(i) to be aligned, we create the corresponding icp-cloud by taking those points in clouds(i) which lie in the spheres defined by the user. This means that the (x,y,z) coordinates of each sphere centre are referred to clouds(0) space and are the same every time we build a icp-cloud; given that the meshes are slightly shifted each other, though, the points lying inside the spheres will (or might, at least) change a little in every clouds(i). We find these shifts with the ICP algorithm and we then apply the resulting transformation matrix to the clouds(i).

4.1.1 ICP Alignment

For each couple [clouds(0), clouds(i)], after the creation of the corresponding icp-clouds, we run the ICP algorithm, which can be resumed as follows:

1. For each P_i^k point in icp-cloud(i), find the nearest point P_0^k in icp-cloud(0);
2. Estimate the roto-translation matrix M which best aligns P_i^k points to the corresponding P_0^k. The matrix is evaluated by calculating the Mean Square Error (MSE) over each point;
3. Apply the transformation matrix M to clouds(i);
4. Repeat from point 1) until a stop criterion is satisfied.

ICP has three stop criteria:

1. A certain number of iteration is reached;
2. The difference between the previous transformation and the current estimated transformation is smaller than a certain value;
3. The sum of Euclidean squared errors is smaller than a defined threshold.

We use both 1 and 3 criteria, by setting 100 as maximum number of iteration and 1^{-8} as threshold for the Euclidean squared errors sum. In Figure 5 we can observe the result of the alignment process between two clouds.

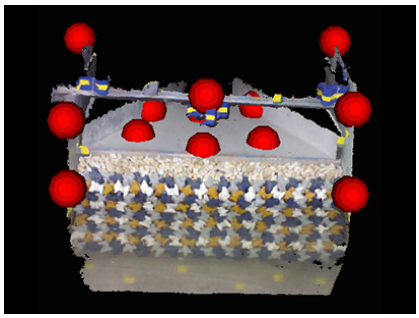

(a) Spheres of points picked by the user

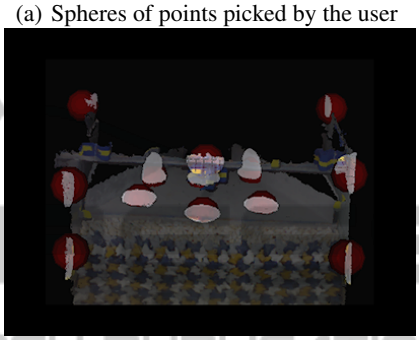

(b) Overlap between the picked spheres and the resulting icp-cloud

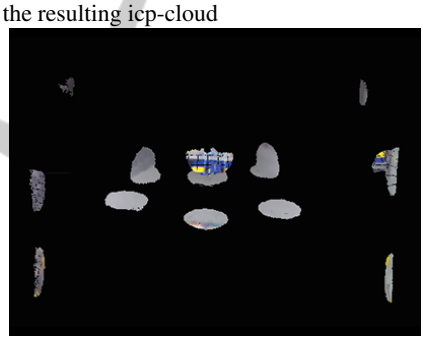

(c) The resulting icp-cloud

Figure 4: icp-cloud for the reference mesh. The user picked some spheres in regions where no movements can occur, such as the bar upon the barrier, the walls and the rod beyond the breakwater (a). The points included in these spheres will populate the icp-cloud. In (b) the reference clouds(0) is superimposed over the points included by the spheres, so that we can observe the points that are extracted to create the icp-cloud, which is shown in (c). The diameter of the spheres can be adjusted and is set by default to 7 centimetres.

4.2 Calculating Accropodes Movements

After the alignment phase, the next step in the workflow is the evaluation of the roto-translation movements of the Accropodes composing the barrier. First, we subsample the reference clouds(0) dividing its space in cubes of side n (which is set by default to 2 centimetres). For each cube j the points contained in it are substituted and represented by their mass centre P_j: we use these P_j as control points to calculate both rotational and translational shifts between the reference cloud and a mesh clouds(i) from the sequence. Figure 6 reports a result of such subsampling process. Every point showed in this mesh represents a control point P_j, that is the mass centre of the points contained in the corresponding j-th cube of the cloud.

4.2.1 Estimate Translation

To estimate translation shifts for a clouds(i), we run a radius search on each mass centre P_j:

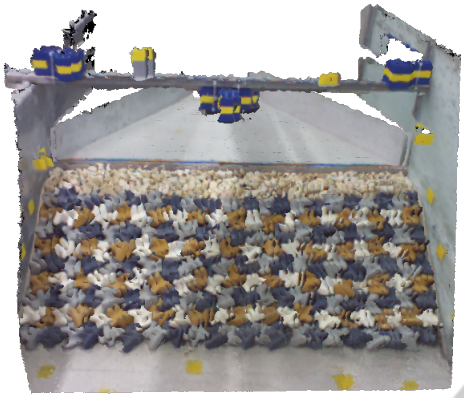

(a) Overlapped 3D models before alignment

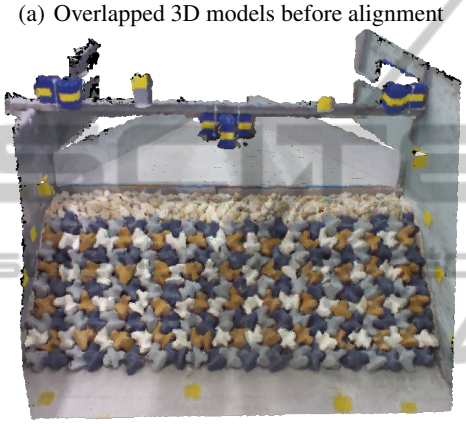

(b) Overlapped 3D models after alignment

Figure 5: Clouds alignment. Before the alignment process, a noticeable shift between the overlapped 3D models is clearly visible. After the alignment, the clouds are perfectly overlapped and the two meshes are not distinguishable.

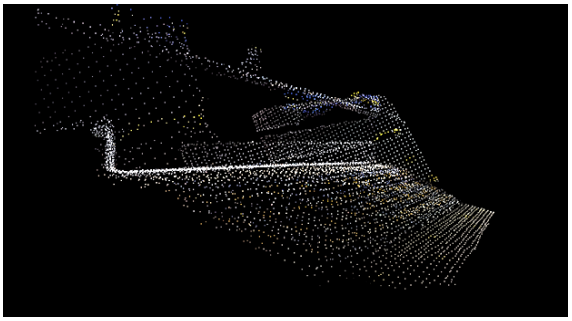

Figure 6: Point Cloud subsampling result.

- For each $P_j = (x_j, y_j, z_j)$, we find in clouds(i) the points lying in the neighbourhood given by the sphere of radius $\frac{n}{2}$ and centre P_j. Let $neighbours(P_j)$ be the set of these points;
- Calculate the mass centre P'_j for the points in $neighbours(P_j)$;
- The movements occurred in the space portion of clouds(i) located by the sphere centred in P_j is given by the Euclidean distance between P_j and P'_j.

We use K-d tree (Bentley, 1975) implementation of PCL library to run radius search over the clouds.

4.2.2 Estimate Rotation

To estimate the rotation of the Accropodes for a clouds(i) we compute surface normals in the mesh. More precisely, to calculate the rotation in a portion of a clouds(i) located by a control point P_j, we proceed as follows:

- Given the point $P_j = (x_j, y_j, z_j)$, estimate in clouds(0) the normal vector $\overrightarrow{N_0}(j)$ of the surface given by the points lying on the spherical neighbourhood of radius $\frac{n}{2}$ and centre P_j;
- Estimate in clouds(i) the normal vector $\overrightarrow{N_i}(j)$ of the surface given by the points lying on the spherical neighbourhood of radius $\frac{n}{2}$ and centre P_j;
- The angle θ between $\overrightarrow{N_0}(j)$ and $\overrightarrow{N_i}(j)$ vectors gives an estimation of the rotation occurred in the portion of clouds(i) located by P_j.

To calculate the angle between $\overrightarrow{N_0}(j) = (A_1, B_1, C_1)$ and $\overrightarrow{N_i}(j) = (A_2, B_2, C_2)$ we calculate the angle between their perpendicular planes, that is:

$$\theta(\overrightarrow{N_0}(j), \overrightarrow{N_i}(j)) = \arccos \frac{|A_1 \cdot A_2 + B_1 \cdot B_2 + C_1 \cdot C_2|}{\sqrt{A_1^2 + B_1^2 + C_1^2} \cdot \sqrt{A_2^2 + B_2^2 + C_2^2}} \quad (1)$$

We estimate normals vector using the method proposed in (Berkmann and Caelli, 1994), which is based on Principal Component Analysis. Figure 7 illustrates an example of normal estimation and comparison for a couple [clouds(0), clouds(i)], considering only a small region of the meshes. Red lines are $\overrightarrow{N_i}(j)$ vectors, while green lines are $\overrightarrow{N_0}(j)$ vectors; the mesh drawn in the picture is the reference cloud. In this example we can see that almost every $\overrightarrow{N_i}(j)$ vector is parallel to the correspondent reference vector $\overrightarrow{N_0}(j)$, since no noticeable movements have occurred in this part of clouds(i).

5 EXPERIMENTAL RESULTS

The resulting software is written in C++ using the Point Cloud Library (PCL) (Rusu and Cousins, 2011), and a Microsoft Kinect device as RGB-D camera. The output of the proposed method of a sequence is a

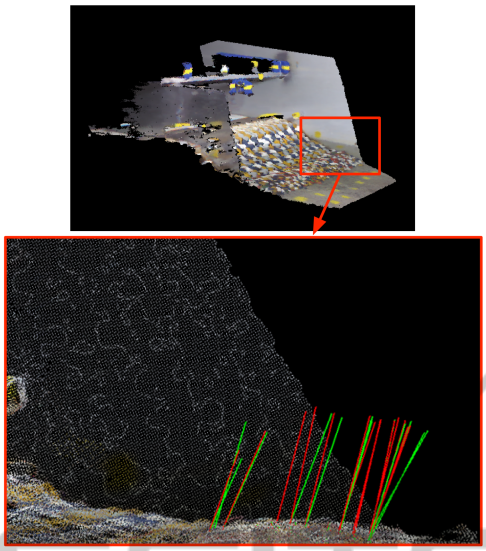

Figure 7: Normals estimation and comparison on a portion of mesh. Green lines are normal vectors computed for the reference cloud, while red lines are normals vectors computed for a following cloud in the sequence. For clarity sake only a subset of vectors is drawn.

text file containing the roto-translation evaluations for each clouds(i). Every j-th line of the file contains the translation and rotation shifts estimated in the spherical neighbourhood of the control point P_j. Every row of the output is then composed of:

- $P_j.x$, $P_j.y$ and $P_j.z$, respectively the x, y, z coordinates of the control point P_j;
- $d(P_j, P'_j)$, distance between P_j and P'_j;
- $\theta(\overrightarrow{N_0}(j), \overrightarrow{N_i}(j))$, angle between normal vectors $\overrightarrow{N_0}(j)$ and $\overrightarrow{N_i}(j)$;
- $\overrightarrow{N_i}(j).x$, $\overrightarrow{N_i}(j).y$, $\overrightarrow{N_i}(j).z$, respectively the x, y, z coordinates of the normal vector $\overrightarrow{N_i}$.

To visually represent the results, we draw contour plots of both translational and rotation values. In order to produce a more readable chart, we plot the values in two dimensions. We are then discarding the z component of the mesh points by projecting the cloud into a two dimensional space; the point of view of such projection is frontal to the scene, and corresponds exactly to the point of view of the Kinect camera. The coordinates of the resulting plane are expressed in centimetres, as well as the colour based legend of the movements.

We can resume the contour plot function with the following equation:

$$contourPlotColour(x,y) \propto d(P_j, P'_j) \qquad (2)$$

where (x,y) are the coordinates of the control point P_j in the two dimensional projection. In the case of rotational movements contour plot, the same holds by substituting in Eq. 2 the distance d by the angle θ between the normals vectors.

Figure 8 shows contour plots of translational movements for a sequence of clouds obtained during an experiment. As we can see, it is possible to easily track the status of the barrier at a glance. As long as waves hit the barrier over time, Accropodes moved increasingly: at the beginning of the test (first three plots of the first row) only few Accropodes moved, whilst at the central and ending phase of the experiment a lot shifted. We can observe that the upper region of the breakwater is the most damaged part.

Figure 9 shows contour plots of rotational movements for the same clouds sequence. These plots, albeit more noisy than the translation shifts plots, contribute to prove an incremental damage of the breakwater. The noise of rotational movements is mainly due to the fact we are estimating normals on very tiny region of the clouds (a sphere with radius of 1 centimetre).

Notice that the proposed monitoring technique allows an immediate understanding of the breakwater conditions over time. The provided series of plots are a precious help for an expert to visually assess the damage of the breakwater in a quick and precise way.

6 CONCLUSIONS AND FUTURE WORKS

The proposed breakwater monitoring method is a good starting point for future improvements. The three dimensional tracking of every single unit of the monitored breakwater is an arduous and stimulating feature that could be investigated: such an ability for a monitoring system does not exist yet, and would be an innovative capacity that would bring coastal engineers to completely new stability analysis techniques.

The monitoring phase of our system is currently offline: users first fulfil the flooding experiment acquiring point clouds used later to evaluate the occurred movements in the breakwater. The stability monitoring of a protection structure requires a constant surveillance and, consequently, a responsive system. The complexity of the involved data processing techniques and the big magnitude of the data itself (3D imaging require big resources to be represented and stored) make real time handling of 3D data an important challenge.

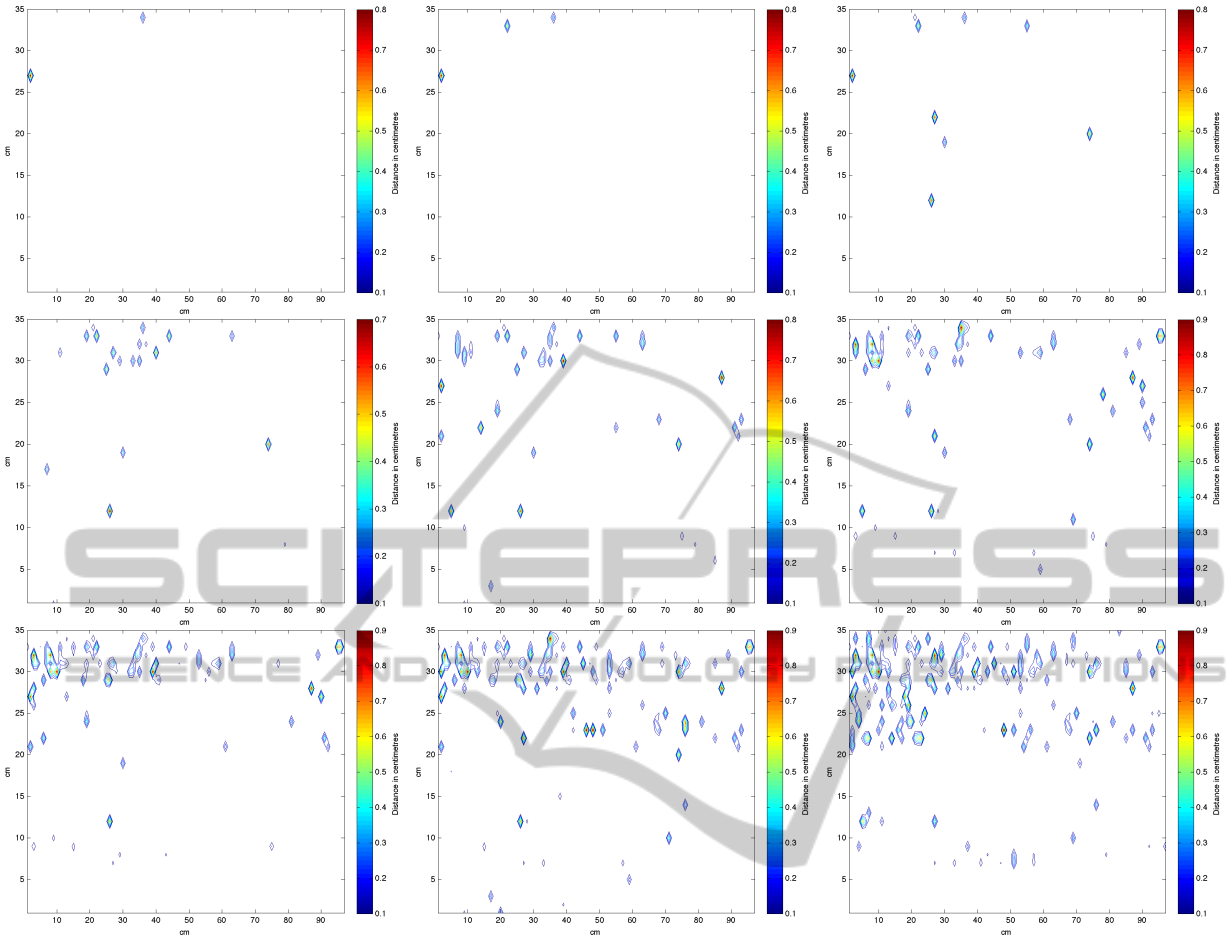

Figure 8: Translation contour plots on X-Y plane from a test sequence (from top left to bottom right).

Application in a Real Scenario

Our system has been designed for laboratory studies, which take place on a controlled scenario considering a scale model. Nevertheless, it is important to highlight that the proposed method and measures are effectively applicable to a real scenario, since the breakwater movements estimation phase is uncoupled from the data acquisition, independently from the considered scale. However, a real world application entails some issues, which represent an interesting case of investigation for future works.

A weather-beaten environment involves intrinsic difficulty. The necessary equipment must be sealed because of wind and water power causing damages. This complicates the point clouds acquisition stage (e.g. stabilization might be needed), but actually doesn't directly affect the calculation of the breakwater units shifts (that is, the movements calculation algorithm would be the same). Despite that, bad light and visibility conditions can cause unclear point cloud reconstruction and lead consequently to an inaccurate evaluation of the movements. This introduces the need of a data processing procedure, aimed at the enhancement of the point clouds for a precise movements calculation.

In our experiments we used a Microsoft Kinect as RGB-D camera to acquire point clouds. Like most of the existing RGB-D cameras, the Kinect infers scene depth by projecting an infrared light pattern (Zhang, 2012). Infrared light is not usable in scenes concerning long distances and, above all, is not usable with sun light. For real world application, hence, other types of RGB-D cameras based on stereo vision techniques must be used (e.g. (Woodfill et al., 2004)). Dealing with bigger scenes does not imply only drawbacks: we have discussed in Section 5 that rotation contour plots suffer a certain amount of noise (see Figure 9), given by the very reduced region where normals are estimated (a sphere with radius of 1 centimetre). In the case of a real breakwater, the calculation of normal vectors would be done by using

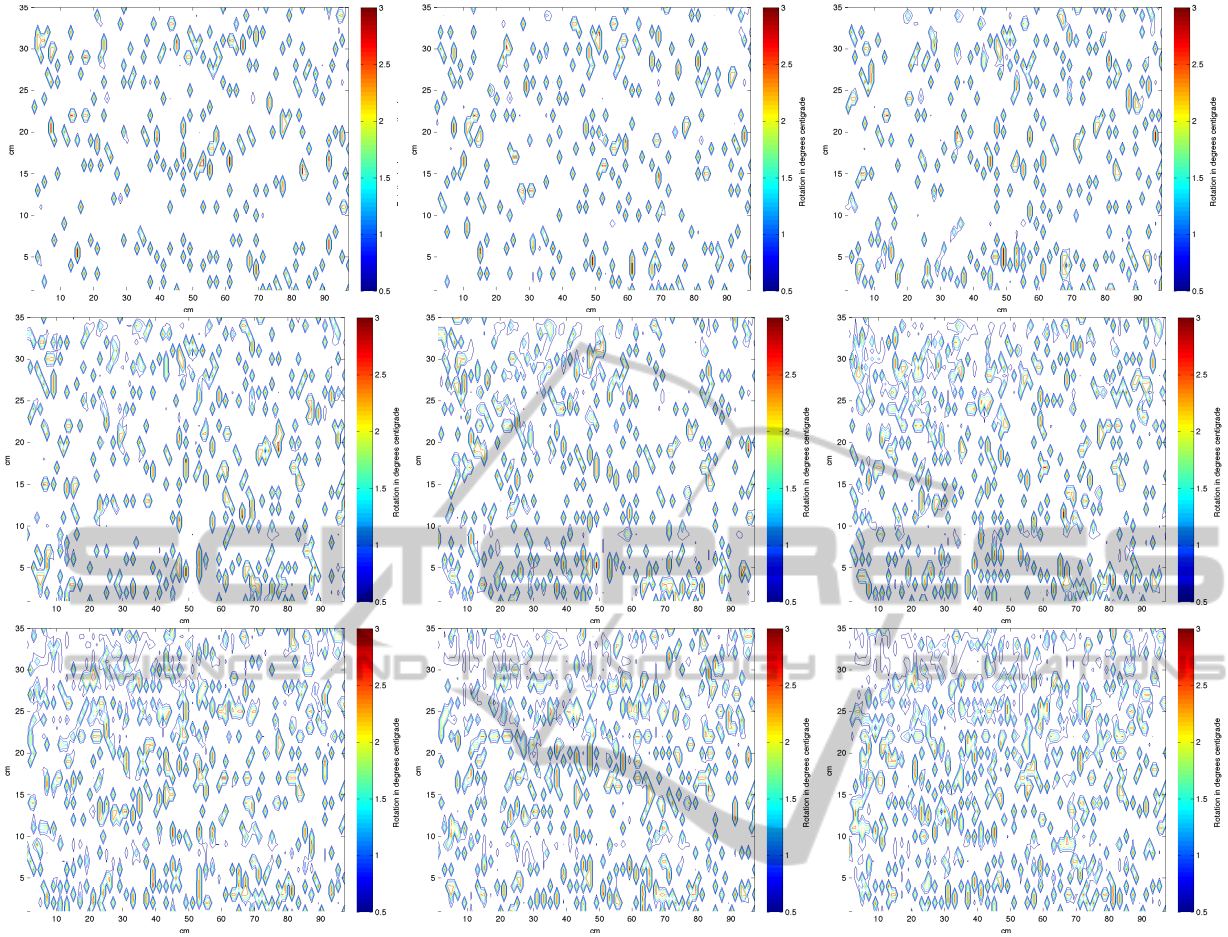

Figure 9: Rotation contour plots on X-Y plane from a test sequence (from top left to bottom right).

much bigger portions of the point cloud: this would make the precision of the normal vector considerably higher, boosting thus the accuracy of the rotation movements monitoring.

REFERENCES

Auld, S. (2010). Innovation in underwater construction: Benefits of real-time 3d imaging. CodaOctopus Products Ltd.

Bentley, J. L. (1975). Multidimensional binary search trees used for associative searching. *Communications of the ACM*, 18(9):509–517.

Berkmann, J. and Caelli, T. (1994). Computation of surface geometry and segmentation using covariance techniques. *Pattern Analysis and Machine Intelligence, IEEE Transactions on*, 16(11):1114–1116.

Caimi, F. M. and Kocak, D. M. (1997). Real-time 3d underwater imaging and mapping using a laser line scan technique. In *Optical Science, Engineering and Instrumentation'97*, pages 241–252. International Society for Optics and Photonics.

Chen, Y. and Medioni, G. (1992). Object modelling by registration of multiple range images. *Image and vision computing*, 10(3):145–155.

Kobayashi, M. and Kaihatsu, S. (1984). Hydraulic characteristics and field experience of new dissipating concrete blocks (ACCROPODE). In *Proceedings of 19th Conference on Coastal Engineering*, Houston, Texas.

Rusu, R. B. and Cousins, S. (2011). 3D is here: Point Cloud Library (PCL). In *IEEE International Conference on Robotics and Automation (ICRA)*, Shanghai, China.

Van der Meer, J. (1987). Stability of breakwater armour layers - Design formulae. *Coastal Engineering*, 11:219–239.

Woodfill, J. I., Gordon, G., and Buck, R. (2004). Tyzx deepsea high speed stereo vision system. In *Computer Vision and Pattern Recognition Workshop, 2004. CVPRW'04. Conference on*, pages 41–41. IEEE.

Zhang, Z. (2012). Microsoft kinect sensor and its effect. *MultiMedia, IEEE*, 19(2):4–10.